Iron nanoparticle driven spin-valve behavior in aligned carbon nanotube arrays

J. D. Bergeson, S. J. Etzkorn, M. B. Murphey, L. Qu, J. Yang et al.

Citation: Appl. Phys. Lett. **93**, 172505 (2008); doi: 10.1063/1.2999374
View online: http://dx.doi.org/10.1063/1.2999374
View Table of Contents: http://apl.aip.org/resource/1/APPLAB/v93/i17
Published by the American Institute of Physics.

Iron nanoparticle driven spin-valve behavior in aligned carbon nanotube arrays

J. D. Bergeson,[1,a)] S. J. Etzkorn,[1] M. B. Murphey,[1] L. Qu,[2] J. Yang,[2,b)] L. Dai,[2] and A. J. Epstein[1,3,c)]
[1]*Department of Physics, The Ohio State University, Columbus, Ohio 43210-1117, USA*
[2]*Department of Chemical and Materials Engineering, University of Dayton, Dayton, Ohio 45469-0240, USA*
[3]*Department of Chemistry, The Ohio State University, Columbus, Ohio 43210-1183, USA*

(Received 20 August 2008; accepted 16 September 2008; published online 28 October 2008)

We report the operation of spin-valve structures formed from arrays of aligned carbon nanotubes. The devices require only one deposited ferromagnetic layer with the embedded iron catalyst nanoparticle serving as the other magnetic electrode. A peak in the resistance occurs clearly as a result of the reversal of the magnetization of the electrodes. Device magnetoresistance ratios reach 25%, yielding an estimate of the spin scattering length of 9 μm at low temperature. © *2008 American Institute of Physics*. [DOI: 10.1063/1.2999374]

While conventional electronic devices manipulate the charge of the electron, spintronic devices[1–3] function by utilizing both the charge and spin of the electron. The spin valve, a principal spintronic device, consists of two magnetic layers separated by a nonmagnetic spacer. These devices operate by injecting spin polarized electrons from one magnetic electrode through the nonmagnetic spacing layer and are analyzed by a second magnetic electrode. The efficacy of such devices is determined by the percentage of spin polarization in the magnetic layers, as well as the loss of electron spin polarization due to spin-flip scattering within the spacing layer and at the interfaces. While much research has been aimed at increasing the spin polarization of the magnetic electrodes, recent work has investigated the use of different materials as the spacing layer including various oxides,[4,5] small molecule organic semiconductors,[6,7] inorganic semiconductors,[8–10] and individual carbon nanotubes (CNTs).[11,12]

Organic materials, with their low spin-orbit coupling and weak hyperfine interaction, are expected to have long spin scattering lengths (l_s) and thus be efficient for transporting spin-polarized electrons. Recent works on organic small molecule thin films report $l_s \sim 200$ nm at 300 K for sexithiophene[6] and $l_s \sim 45$ nm at 11 K for tris-(8-hydroxyquinoline) aluminum.[7] Pioneering research[11] demonstrated spin-dependent transport in an individual CNT by locating isolated tubes lying on a substrate surface and lithographically contacting the sidewalls with magnetic electrodes. However, the isolation and electrical contact of an individual CNT is a difficult and time consuming task. Since this discovery, the chemistry of CNTs has matured, and CNTs can now be readily created in the form of large scale aligned arrays.[13–15] These aligned arrays can be lithographically patterned and show potential for electronic applications without the need for direct manipulation on the nanoscale.

Here we report spin-dependent transport through aligned vertical arrays of multiwalled CNTs (MWNTs) that use magnetic nanoparticles as one electrode. Samples are prepared with only one thin film magnetic electrode, using the magnetic catalyst nanoparticle formed during the growth of the MWNT array as the other magnetic electrode. A strong hysteretic magnetoresistance (MR) plateau indicative of typical spin-valve behavior is observed with switching corresponding to the independent reversal of each magnetic electrode. The data show that spin coherence is largely maintained throughout the entire length (~ 7 μm) of the CNT array, with an estimate giving $l_s \sim 9$ μm.

CNT arrays are formed by pyrolysis of iron (II) phthalocyanine (FePc) under Ar/H_2 atmosphere at 800–1100 °C using quartz substrates in a flow reactor.[15] In this method, the FePc provides both the Fe nanoparticle catalyst, which serves as a magnetic electrode in the completed device, and the necessary carbon to support tube growth. The resultant MWNT array is highly vertically aligned [Fig. 1(a)] and relatively dense. By varying the conditions for nanotube growth, the Fe nanoparticle can be introduced at the top and/or bot-

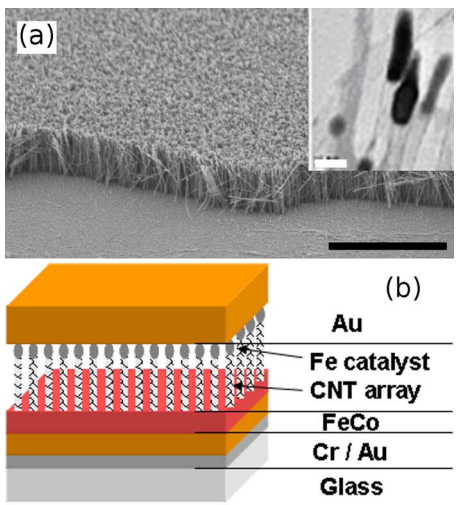

FIG. 1. (Color online) (a) SEM image of the as-deposited CNT array on the quartz substrate (scale bar: 20 μm). Inset: corresponding TEM image of the iron particle capped MWNT (scale bar: 50 nm). (b) Schematic representation of the device, note the Fe catalyst particle (upper tips of the CNT) formed during the deposition of the CNT array serves as the second FM layer in the spin-valve structure.

[a)]Present address: National Renewable Energy Laboratory, Golden, CO 80401, USA.
[b)]Present address: Argonne National Laboratory, Argonne, IL 60439, USA.
[c)]Author to whom correspondence should be addressed. Electronic mail: epstein@mps.ohio-state.edu.

tom of the nanotube tip(s).[16] For the samples prepared in this study, the Fe nanoparticles are embedded in the upper tips of the as-deposited CNT array [inset, Fig 1(a)]. Typically, MWNT with outer diameters in the range of 20–50 nm and tube lengths of ~5–20 μm were prepared.[16,17]

Following the array growth, a thick layer of gold is deposited to provide electrical contact to the upper tips of the MWNT, which have the embedded Fe nanoparticles. In order to electrically contact the lower end of the MWNT, the array is removed from the quartz substrate by one of the following two methods: treatment with hydrofluoric acid (HF)[15] or mechanical removal using a commercially available double-sided conducting tape.[17] Both methods will remove the Fe catalysts from MWNT lower ends if any, which has been confirmed by scanning electron microscopy (SEM) and transmission electron microscopy (TEM). However, such removal (especially the HF treatment) often causes nanotube clustering and the development of voids within the previously dense array. These micron-sized voids allow for direct shorts to the gold layer when attempts are made to directly deposit a second ferromagnetic (FM) electrode using vacuum evaporation. Thus, thin films of chromium (10 nm), gold (30 nm), and iron-cobalt ($Fe_{50}Co_{50}$, 8nm) are deposited on a glass substrate. Contact with the exposed, lower tips of the MWNT array is made by employing a pressure contact with the magnetic FeCo layer. All deposition and handling of the FeCo films and device assembly are performed in an inert atmosphere. A schematic representation of the device is shown in Fig. 1(b).

The CNT-encapsulated Fe nanoparticles [inset, Fig. 1(a)] are typically only slightly smaller than the diameter of the MWNT[16] yet larger than the superparamagnetic critical size for iron (~10 nm). Measurements of magnetization versus applied field [Fig. 2(a)] show that the Fe catalyst particles exhibit a hysteresis at 4.5 K with a coercivity of 200 mT, much larger than that of the FeCo layer (~20 mT) [inset Fig. 2(a)]. An investigation of the magnetic properties demonstrates that the catalyst particles still behave as FM at 300 K, with a coercive field of approximately 5 mT providing the potential for room temperature operation. The particle size and enhanced coercivity suggest possible single domain behavior for each Fe nanoparticle. The large difference in coercive field between the two magnetic layers enables a stable antialigned state over a relatively large range in applied field without the use of an antiferromagnetic pinning layer.

At low temperatures, the resistance of the Fe nanoparticle/CNT array/FeCo device depends on the relative alignment of the magnetizations of the magnetic electrodes, i.e., the parallel magnetization resistance R_p differs from the resistance for antiparallel alignment R_{ap}, indicative of the spin-valve effect shown in Fig. 2(b) (top), with a MR ratio defined as $MR=(R_{ap}-R_p)/R_p$. The device is cooled in zero applied magnetic field from 300 to 4.5 K for measurements. Resistance is measured versus applied magnetic field using a Quantum Design Physical Properties Measurement System in a two-terminal configuration at various applied bias currents (i_B) ranging from 5 to 500 nA. The applied magnetic field is first swept from +1 to −1 T and then back to +1 T with resistance measured at regular intervals. The device shows a clear hysteretic on/off state with the switching fields consistent with the measured coercive fields of the Fe catalyst particle and the FeCo layer. We observe MR values up to

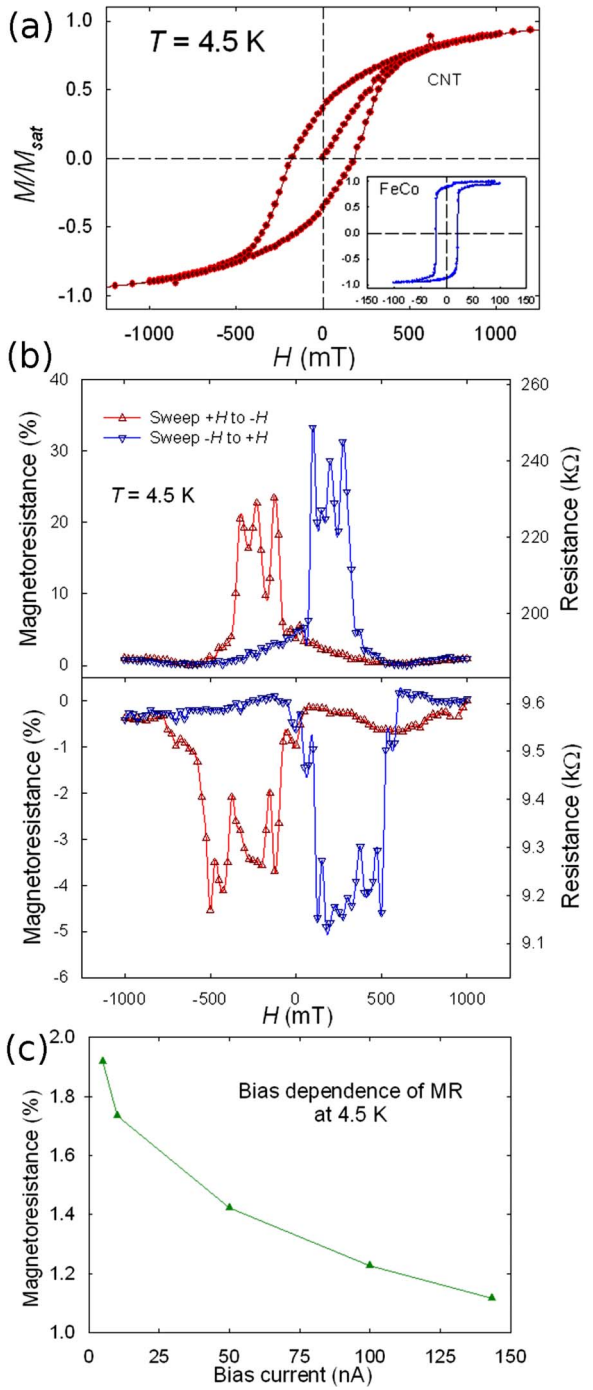

FIG. 2. (Color online) (a) Magnetic hysteresis data of the CNT array after removal from the quartz substrate showing a sizeable coercive field at 4.5 K. Inset shows the hysteresis of the deposited FeCo film on a glass substrate. (b) MR—defined as $(R_{ap}-R_p)/R_p$—(left axis) and resistance (right axis) vs field for (top) (Fe nanoparticle)/CNT array/FeCo device at 4.5 K and 50 nA bias current and (bottom) a second device with an oxidized FeCo layer, at 4.5 K and 500 nA bias current. (c) Bias current dependence on MR of a third device showing an increase in the magnitude of the effect at lower bias currents.

~25% (with i_B=50 nA). This MR value is comparable to reported values in individual MWNT at much lower bias currents (i_B~0.5 nA).[18,19] Thus the large observed MR may reflect the 50 nA current being distributed among numerous MWNT in the array. The switching of MR within the array is observed as a sharp effect with respect to field, indicating that the magnetization directions of the Fe nanoparticles switch as an ensemble. It is noted that theoretical calcula-

tions predict an increase in MR for CNT with multiple conducting pathways due to electron wave interference.[20]

We can estimate the spin scattering length for electrons traveling in the CNT array using Julliere's model[21] for tunneling MR, where the difference between the parallel and antiparallel resistance states is

$$\Delta R/R_p = (R_{ap} - R_p)/R_p = 2P_1P_2/(1 + P_1P_2), \quad (1)$$

where P_1 and P_2 are the spin polarizations of the injecting electrodes, in our case Fe ($P_1 \sim 44\%$) and FeCo ($P_2 \sim 55\%$).[22] For the device in Fig. 2(b) (top), $\Delta R/R_p$ averages to ~19%, reaching a maximum of ~25%. Given a length of the CNT array of 7 μm as determined from SEM images, and assuming the spin polarization reduces as $\exp(-l/l_s)$,[11] for $\Delta R/R_p = 20\%$ we estimate $l_s = 9$ μm at 4.5 K. This value is much larger than the initial low-temperature estimate of 130 nm reported for individual MWNT[11] and even the 1.5 μm estimated for an individual single-walled CNT (SWNT).[23] The value reported here is also more consistent with values reported for the electron scattering length (>1 μm) in CNT[24,25] at room temperature. The low atomic number of carbon reduces the spin-orbit interaction and, having no hydrogen atoms, spin scattering due to the hyperfine interaction should be nearly negligible, which should allow for a much longer spin scattering length than estimated here. However, much of the loss of spin coherence likely occurs at the interfaces, which makes the practical realization of the estimated $l_s \sim 1$ cm from low-temperature electron spin resonance measurements[26] difficult to achieve in spintronic devices.

For some devices, the FeCo layer is allowed to oxidize under ambient laboratory atmosphere for 7–10 days. In these cases, a negative MR [Fig. 2(b), bottom] often is observed. This type of inversion has been reported in other magnetic tunnel junctions and is attributed to the FM/oxide interface.[4,5] It is noted that some devices with this oxidation step retained the positive MR observed with the unoxidized FeCo layer. This variability in sign of MR may reflect the sensitivity of the pressure contact at the FeCo/MWNT interface and/or variability of the oxide layer formed. Additionally, some devices are prepared with a small (~1.5 nm) AlO_x layer to introduce a deliberate insulating oxide barrier. Such samples also exhibit a similar but larger negative (~−7%) MR.[27] This variance in both sign and magnitude in CNT MR has been reported for other unoxidized systems as well[28] and may be tunable via gating.[29]

There is a strong increase in magnitude of MR as the bias current is decreased [Fig. 2(c)]. Similar behavior has been reported for individual SWNT and MWNT.[18,23] An increase of this type has been attributed to tunneling processes,[19] Coulomb blockade,[23] and other excitations.[30] This increase in MR with decreasing i_B is consistent with the tunneling spectra observed in similar CNT arrays at cryogenic temperatures.[31] We suggest that any tunneling that does occur is at one or both of the ferromagnet/CNT interfaces. Our estimation of l_s suggests that the transport would be nearly ballistic through the length of the CNT. In both oxidized and unoxidized cases, the *I-V* curve is determined to be linear, corresponding to behavior of devices fabricated with individual MWNT.[28]

We have shown MWNT arrays incorporating magnetic catalyst nanoparticles efficiently transport spin in spin-valve devices exhibiting MR up to 25%, with an estimated spin scattering length of 9 μm.

This work is supported in part by DOE Grant Nos. DE-FG02-86ER45271 and DE-FG02-01ER45931, and AFOSR Grant Nos. FA9550-06-1-0175 and FA9550-06-1-0384, NSF Grant No. CMS-0609077, and IMR Grant Nos. FG0004 and FG0036. The support of the Materials and Manufacturing Directorate of the Air Force Research Laboratory is gratefully acknowledged. Thanks also to L. Li for his assistance.

[1] G. A. Prinz, Science **282**, 1660 (1998).
[2] S. A. Wolf, D. D. Awschalom, R. A. Buhrman, J. M. Daughton, S. von Molnár, M. L. Roukes, A. Y. Chtchelkanova, and D. M. Treger, Science **294**, 1488 (2001).
[3] I. Zutic, J. Fabian, and S. Das Sarma, Rev. Mod. Phys. **76**, 323 (2004).
[4] J. M. De Teresa, A. Fert, J. P. Contour, F. Montaigne, and P. Seneor, Science **286**, 507 (1999).
[5] M. Sharma, S. X. Wang, and J. H. Nickel, Phys. Rev. Lett. **82**, 616 (1999).
[6] V. Dediu, M. Murgia, F. C. Matacotta, C. Taliani, and S. Barbanera, Solid State Commun. **122**, 181 (2002).
[7] Z. H. Xiong, D. Wu, Z. V. Vardeny, and J. Shi, Nature (London) **427**, 821 (2004).
[8] S. Crooker, M. Furis, X. Lou, C. Adelmann, D. L. Smith, C. J. Palmstrøm, and P. A. Crowell, Science **309**, 2191 (2005).
[9] I. Appelbaum, B. Huang, and D. J. Monsma, Nature (London) **447**, 295 (2007).
[10] B. T. Jonker, G. Kioseoglou, A. T. Hanbicki, C. H. Li, and P. E. Thompson, Nat. Phys. **3**, 542 (2007).
[11] K. Tsukagoshi, B. W. Alphenaar, and H. Ago, Nature (London) **401**, 572 (1999).
[12] L. E. Hueso, J. M. Pruneda, V. Ferrari, G. Burnell, J. P. Valdés-Herrera1, B. D. Simons, P. B. Littlewood, E. Artacho, A. Fert, and N. D. Mathur, Nature (London) **445**, 410 (2007).
[13] L. Dai, A. Patil, X. Gong, Z. Guo, L. Liu, Y. Liu, and D. Zhu, ChemPhysChem **4**, 1150 (2003), and references cited therein.
[14] L. Qu, Q. Peng, L. Dai, G. Spinks, G. Wallace, and R. H. Baughman, MRS Bull. **33**, 215 (2008), and references cited therein.
[15] S. M. Huang, L. M. Dai, and A. W. H. Mau, J. Phys. Chem. B **103**, 4223 (1999).
[16] D. C. Li, L. Dai, S. Huang, A. W. H. Mau, and Z. L. Wang, Chem. Phys. Lett. **316**, 349 (2000).
[17] J. Yang, L. Dai, and R. A. Vaia, J. Phys. Chem. B **107**, 12387 (2003).
[18] B. Zhao, I. Mönch, H. Vinzelberg, T. Mühl, and C. M. Schneider, Appl. Phys. Lett. **80**, 3144 (2002).
[19] B. Zhao, I. Mönch, H. Vinzelberg, T. Mühl, and C. M. Schneider, J. Appl. Phys. **91**, 7026 (2002).
[20] S. Kokado and K. Harigaya, Phys. Rev. B **69**, 132402 (2004).
[21] M. Julliere, Phys. Lett. **54**, 225 (1975).
[22] J. S. Moodera, J. Nassar, and G. Mathon, Annu. Rev. Mater. Sci. **29**, 381 (1999).
[23] J. R. Kim, H. M. So, J. J. Kim, and J. Kim, Phys. Rev. B **66**, 233401 (2002).
[24] S. Frank, P. Poncharal, Z. L. Wang, and W. A. de Heer, Science **280**, 1744 (1998).
[25] J. Y. Park, S. Rosenblatt, Y. Yaish, V. Sazonova, H. Ustunel, S. Braig, T. A. Arias, P. Brouwer, and P. L. McEuen, Nano Lett. **4**, 517 (2004).
[26] B. Alphenaar, S. Chakraborty, and K. Tsukagoshi, in *Electron Transport in Quantum Dots*, edited by J. P. Bird (Kluwer Academic, New York, 2003), Chap. 11.
[27] See EPAPS Document No. E-APPLAB-93-077841 for a figure of negative MR in a CNT array device with an AlO_x tunnel barrier. For more information on EPAPS, see http://www.aip.org/pubservs/epaps.html.
[28] R. Thamankar, S. Niyogi, B. Y. Yoo, Y. W. Rheem, N. V. Myung, R. C. Haddon, and R. K. Kawakami, Appl. Phys. Lett. **89**, 033119 (2006).
[29] B. Nagabhirava, T. Bansal, G. U. Sumanasekra, and B. W. Alphenaar, Appl. Phys. Lett. **88**, 023503 (2006).
[30] T. S. Santos, J. S. Lee, P. Migdal, I. C. Lekshmi, B. Satpati, and J. S. Moodera, Phys. Rev. Lett. **98**, 016601 (2007).
[31] D. N. Davydov, J. Li, K. B. Shelimov, T. L. Haslett, M. Moskovits, and B. W. Statt, J. Appl. Phys. **88**, 7205 (2000).